

pH-Dependent Selective Protein Adsorption into Mesoporous Silica

Sebastian T. Moerz[†] and Patrick Huber^{*,†}

Institute of Materials Physics and Technology, Hamburg University of Technology (TUHH), D-21073 Hamburg-Harburg, Germany, and Experimental Physics, Saarland University, D-66041 Saarbruecken, Germany

E-mail: patrick.huber@tuhh.de

Abstract

The adsorption of lysozyme, cytochrome *c* and myoglobin, similar-sized globular proteins of approximately 1.5 nm radius, into the mesoporous silica material Santa Barbara Amorphous-15 (SBA-15) with 3.3 nm mean pore radius has been studied photometrically for aqueous solutions containing a single protein type and for binary protein mixtures. Distinct variations in the absolute and relative adsorption behavior are observed as a function of the solution's pH-value, and thus pore wall and protein charge. The proteins exhibit the strongest binding below their isoelectric points pI, which indicates the dominance of electrostatic interactions between charged amino acid residues and the -OH groups of the silica surface in the mesopore adsorption process. Moreover, we find for competitive adsorption in the restricted, tubular pore geometry that the protein type which shows the favoured binding to the pore wall can entirely suppress the adsorption of the species with lower binding affinity, even though the latter would adsorb quite well from a single component mixture devoid of the strongly binding protein. We suggest that this different physicochemical behavior along with the large specific surface and thus adsorption capability of mesoporous glasses can be exploited

for separation of binary mixtures of proteins with distinct pI by adjusting the aqueous solution's pH.

Introduction

Over the last decades much attention has been paid to the adsorption and immobilization of charged, complex molecules at planar surfaces and in porous materials.^{1–17} Especially nano- or more strictly spoken mesoporous materials and their interaction with biomolecules have been in the focus of intensive research, since they combine a high inner surface area with pore sizes large enough to comfortably host most proteins and enzymes.^{2,10} The analogies between artificial nanopores and biological transport pores in biomembranes^{18,19} and the existence of biomaterials consisting of proteins embedded in mesoporous matrixes^{20,21} has also stimulated fundamental studies on biomolecular adsorption, diffusion, and translocation processes in such geometric confinement.^{22–27} Moreover mesoporous media promise a vast variety of applications in biochemical technologies, like enzymatic catalysis^{10,28,29}, protein crystallization^{30,31} and the fractionation of biological fluids like blood into their individual components.³² New means of targeted drug delivery^{2,33–38} and drug design³⁹, biosensors^{40–44} and nanocomposite materials⁴⁵ can be envisaged. The optical transparency of mesoporous glasses along with the robustness of the fluidity of liquids at the nanoscale^{46–48} allows one to employ them as versatile subunits in Lab-on-a-chip⁴⁹ or more gener-

*To whom correspondence should be addressed

[†]Institute of Materials Physics and Technology, Hamburg University of Technology (TUHH), D-21073 Hamburg-Harburg, Germany

[‡]Experimental Physics, Saarland University, D-66041 Saarbruecken, Germany

ally spoken microfluidic systems.^{50–53} Electrically conductive nanoporous solids, such as nanoporous gold or nanoporous carbon, additionally allow one to reversibly change the fluid/pore wall interaction by the application of electrical potentials and thus permit a versatile, external control of adsorption, guest-host interaction and fluid flow processes.⁵⁴

Especially the separation of a single protein type from a mixture containing a multitude of different biomolecules is of great importance for science as well as for technical applications. Three prominent ways to facilitate such a fractionation are dialysis, filtration and chromatography. While adsorption of proteins does not play a role in dialysis, it can be exploited to customise filtration applications⁵⁵ and selective adsorption is the fundamental principle behind chromatography.

An obvious way to separate a protein mixture is mere size-selectivity.^{56–58} When the pores of a filtering membrane are too small for one protein type to enter, but large enough for a second to pass, forcing the solution to flow or diffuse through the membrane will restrain the larger type.^{51,59,60} Successful size-selective separation of a binary protein mixture has been demonstrated by Katiyar *et al.*⁶¹ This study shows that the pores of the host material have to be slightly larger than the hydrodynamic radius of the protein to ensure adsorption. Yet mere size-exclusion is not the only factor determining the selective adsorption from multi-component solutions: Both the pore size and the protein-surface interaction play a crucial role in selective adsorption.⁶² For example, electrostatic exclusion from the membrane is another means of filtration and can be used to separate two protein types of similar size but different net charge. A combination of protein adsorption and subsequent size-selective filtration was published by Causserand *et al.*⁵⁵ in 2001.

In this study, we use the mesoporous silica material Santa Barbara Amorphous-15 (SBA-15) to explore the competitive adsorption from binary mixtures of lysozyme, cytochrome *c* and myoglobin. These three proteins have similar hydrodynamic radii of approx. 1.5 nm as estimated from small-angle X-ray scattering experiments^{10,63} and their comparable molecular mass. They fit comfortably into the SBA-15 pores, thus size-selectivity is unlikely to play any role.

As shown in previous studies¹⁰ the adsorption of native proteins in low ionic strength solutions is dominated by electrostatic interaction between charged amino acid residues and the -OH groups of the silica surface. This attractive interaction competes with the coulombic repulsion between equally charged protein molecules. At the isoelectric point, where the overall charge of the protein vanishes, this repulsion becomes negligible, the protein-silica interaction is dominated by van-der-Waals as well as polar interactions and a dense packing of molecules into the pores is observed.⁶⁴ While similar in size, the three proteins used in this study differ in their respective isoelectric points. We demonstrate that this different physicochemical behavior results in a distinct adsorption behavior as a function of pH.

Experimental

SBA-15 preparation and characterization

The synthesis of hexagonally ordered mesoporous SBA-15 was first reported by Zhao *et al.*⁶⁵ The samples used in this thesis were prepared according to the following procedure: We mix 4 g of the tri-block co-polymer PEO₂₀-PPO₇₀-PEO₂₀ with 129.6 g water and 19.3 ml HCl (37%). Due to its amphiphilic nature, the polymer forms an ordered phase of micellar structures when mixed with water. Vigorous stirring at 350 rpm for four hours is needed to ensure a homogenous emulsion. The mixture is kept in an oil bath at 55 °C during this process. We then add 8.65 g tetraethylorthosilicate and stir the system for another 20 hours. We subsequently increase the temperature to 85 °C and let the mixture rest for another 22 hours without stirring. During this time, the silicon from the TEOS leads to an accumulation of silica around the polymer micelles. These aggregates precipitate as a fine-grained powder. Calcination of the repeatedly rinsed powder at 500 °C finally removes the polymer while preserving a negative of the micellar structure in the silica grains. The porous silica powder can now be used without further treatment or purification.

The as-prepared SBA-15 was characterised by

measuring volumetric nitrogen sorption isotherms in a custom-made, all-metal gas handling system.

The isotherms were analysed using the mean-field model for capillary condensation proposed by Saam and Cole^{66, 67} This yields a bimodal pore size distribution consisting of a broad Gauss peak ($r_{\text{micro}} = 0.75$ nm with $\sigma_{\text{micro}} = 78\%$) corresponding to a pronounced microporosity⁶⁸ and a narrower peak ($r_{\text{meso}} = 3.3$ nm with $\sigma_{\text{meso}} = 6.5\%$) which is attributed to cylindrical nanopores. A BET analysis of the sorption isotherms yields a specific inner surface of 613.9 m²/g. Small angle x-ray diffraction reveals a hexagonal arrangement of these mesoporous channels with a lattice parameter $a_h = 10.71 \pm 0.08$ nm.^{69,70} Since the molecules studied here are far too large to enter the micropores, the microporous fraction of the samples was neglected in this study.

We have not performed pH-dependent measurements of the ζ -potential of SBA-15 and thus of the charging of the mesoporous particles. Given its importance for adsorption processes in water⁷¹, there is, however, sizeable literature available with regard to the pH-dependence of the ζ -potential of silica surfaces⁷² and of SBA-15 in particular.⁷¹ For the considerations following below, it is interesting to note that the isoelectric point of SBA-15 has been reported as pH 3.8.⁷³

Proteins

Bovine heart cytochrome *c* (purity $\geq 95\%$, catalog number C2037), equine skeletal muscle myoglobin (purity 95-100%, catalog number M0630) and chicken egg white lysozyme (purity $\geq 90\%$, catalog number L6876) were purchased from Sigma Aldrich and used without further treatment or purification. According to the distributor, the proteins' masses are 12.3 kDa, 17.6 kDa and 14.3 kDa and the isoelectric points pH 10.0-10.5, pH 7.3 and pH 11.35, respectively.

Buffer solutions

10mM buffers were prepared according to the following recipes: pH 3.0 (116.37 g of 0.01 M citric acid and 4.0 ml of 0.01 M trisodium citrate), pH 3.8 (200.02 g of 0.01 M acetic acid and 15 ml of 0.01 M sodium acetate), pH 4.5 (100.23 g of

0.01 M trisodium citrate and 120 ml of 0.01 M citric acid), pH 6 (100.14 g of 0.01 M monopotassium phosphate and 32.5 ml of 0.01 M sodium hydroxide), pH 7.3 (50.40 g of 0.01 M sodium hydroxide and 41.7 ml of 0.05 M monopotassium phosphate), pH 8.5 (83 ml of 0.01 M sodium tetraborate and 13.1 ml of 0.01 M hydrochloric acid) and pH 10.6 (100 g of 0.01 M sodium bicarbonate and 71 ml of 0.01 M sodium hydroxide). PH values were calibrated using a *Mettler Toledo Seven Easy* pH meter equipped with an *InLab Expert Pro* electrode.

Protein adsorption experiments

Single protein solutions containing 2 g/L of a single protein and binary mixtures containing two different proteins with 1 g/L each were prepared with the buffers described above. Small amounts of SBA-15 (4.0 – 9.0 mg, measured with a *Sartorius type 1801* analytical balance) were mixed with appropriate amounts of protein solution (200 μ l per mg of SBA-15) and transferred to *Eppendorf Safe-Lock* tubes. The silica powder was dispersed by ultrasonification for 10 minutes. The tubes were equipped with small stirring bars and transferred to a water bath kept at 31°C. Both the bath and the samples were stirred at 350 rpm using an *IKA RCT basic safety control* magnetic stirrer. The samples were kept in the bath for five days, which was found to be sufficient to reach equilibrium.^{74,75,76} The protein concentrations in the supernate were determined photometrically. UV-Vis absorbance spectra were recorded with an *Ocean Optics USB2000-UV-VIS-ES* spectrometer and a *DT-MINI-2-GS UV-VIS-NIR* light source. The light source uses a deuterium and a halogen bulb to provide a continuous spectrum ranging from 200 to 850 nm. The spectrometer and the light source were connected to a cuvette holder via appropriate fiber optics. Disposable semi-micro UV-cuvettes (*Brand*, cat. no. 7591 50.) held the sample aliquots during the photometrical analysis. Note that we found no hints for protein degradation in UV-Vis absorbance spectra over time periods typical for our experiments (120 hours). This is maybe not too surprising given the small, globular character of the molecules studied here. The individual supernate concentrations after the adsorption were

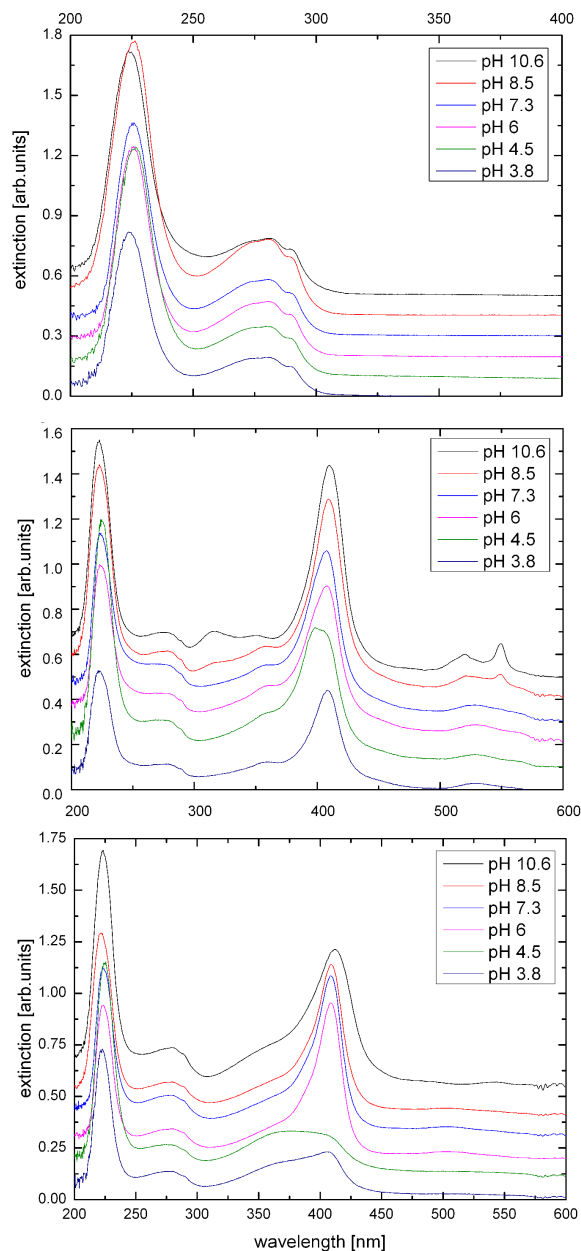


Figure 1: Reference spectra of the three different proteins at different pH, shifted with a vertical offset for better visibility. Top : Lysozyme. Middle: Cytochrome *c*. Bottom: Myoglobin.

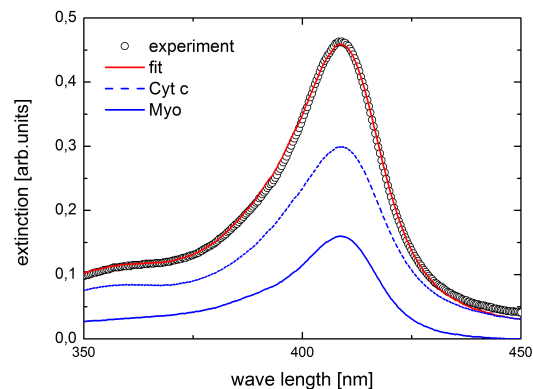


Figure 2: Linear deconvolution of a UV-Vis spectrum of the supernate after competitive adsorption of cytochrome *c* and myoglobin at pH=6. Plotted are the experimental data along with the reference spectra of the single proteins weighted according to their contribution and the corresponding sum spectrum (fit).

calculated by performing a multiple linear regression of the supernate spectrum $\alpha_S(\lambda)$

$$\alpha_S(\lambda) = c_1 \cdot \alpha_A(\lambda) + c_2 \cdot \alpha_B(\lambda) \quad (1)$$

using the respective reference spectra α_A and α_B of the mixtures' two components and their concentrations c_1 and c_2 in units of gram per litre. The reference spectra of the three different proteins recorded at different pH values are shown in Figure 1. In Fig. 2 a deconvolution of a supernate spectrum is exemplified. Finally, the amount of adsorbed protein per gram of the mesoporous host material was calculated from the difference of the initial and final protein concentrations.

Results and discussion

As shown in the top panel of Figure 1 the spectrum of lysozyme was independent of the pH value except for the most alkaline buffer. The cytochrome *c* data are shown in the middle panel. Above pH 8.5 the distinct peaks in the Q band region between 500 and 550 nm indicate a change in the protein's oxidation state from ferric to ferrous.⁷⁷ However, this transition should not affect our experiments, since the oxidation state has no significant influence on the adsorption behavior of folded

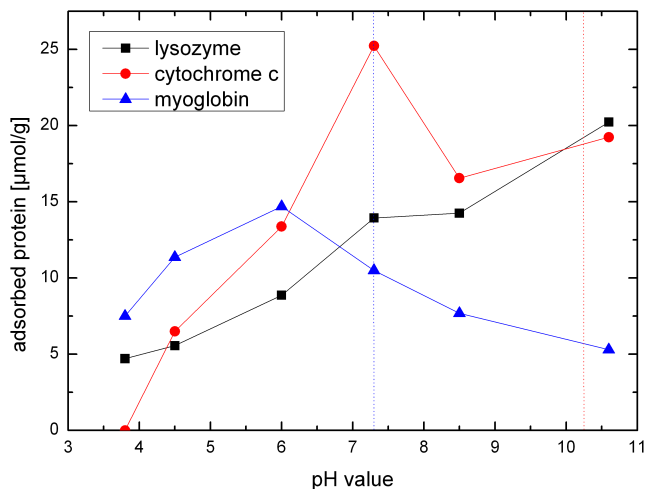


Figure 3: Maximum pore loading of SBA-15 for lysozyme (black squares), cytochrome *c* (red circles) and myoglobin (blue triangles) for different pH values in 10 mM buffer solutions.

cytochrome *c*.⁷⁸ Cytochrome *c* appears to be stable for all pH values. The broadening and blue-shift of the Soret band of the pH 4.5 sample indicates a transition of the central iron ion from a low-spin to a high-spin state and is not a sign of a larger structural change.⁷⁷ The Soret peak of myoglobin exhibits a broadening for both high and low pH values. Nevertheless, we used these spectra to calculate the supernate concentration according to equation ???. To estimate the maximum pore loading of the different proteins at the examined pH values, we mixed SBA-15 samples with solutions containing 2 g/L of the respective protein. Based on our previous findings⁷⁴ we assume that this initial concentration is sufficient to estimate the saturation value of the Langmuir-type isotherms. The adsorption was carried out as described above.

In Figure 3 we show the measured maximum pore loadings in μmol per gram of SBA-15 as a function of the buffer pH. The black squares represent the lysozyme data, while the red circles and blue triangles denote cytochrome *c* and myoglobin, respectively. Neither protein showed any adsorption at pH 3 where both the surface and the protein have the same charge sign.⁷³ The pH 3 buffer is therefore neglected for the following measurements. The maximum of lysozyme adsorption is beyond the scope of the pH values investigated, as is its isoelectric point. Both cytochrome *c* and myoglobin exhibit clear max-

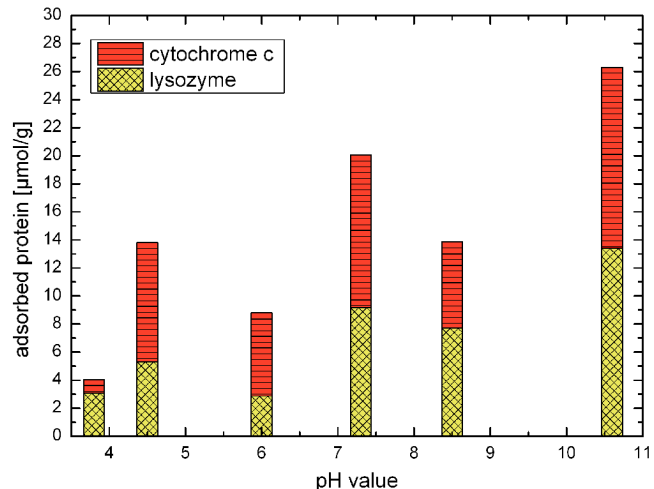


Figure 4: Proteins adsorbed to SBA-15 from a binary mixture of cytochrome *c* and lysozyme.

ima considerably below their isoelectric points, which are indicated by the vertical blue dotted line (myoglobin) and the red dotted line (cytochrome *c*). Myoglobin still shows a non-neglectable pore loading even in the most alkaline buffers where strong electrostatic repulsion between the protein and the surface is expected. The observed adsorption can be explained by positively charged patches on the protein's surface which are present despite the molecule's negative overall charge. Interfacial charge regulation may also contribute to an attractive interaction even above the pI.⁷⁹

With respect to the pH-dependent adsorption of the proteins the stability of mesoporous SBA-15 in aqueous solution should be discussed. Pham *et al.*⁸⁰ performed a thorough study of the dissolution of SBA-15 as a function of pH. They find that this matrix is increasingly unstable for pH values larger than 7. E.g. in their column experiments, more than 45% of the initial SBA-15 dissolved within 48 hours, when a pH 8.5 solution flowed through the column. In our experiments, where the mesoporous silica is exposed to the solution for more than 120 hours, we found no hints for a dissolution of the matrix in the alkaline regime. This may be related to the fact that, in contrast to the experiments by Pham *et al.*, we did not permanently exchange the solution. Moreover, the protein adsorption possibly reduces the silica degradation process in the alkaline regime.

The bar graph in Figure 4 shows the resulting pore loadings from competitive adsorption from

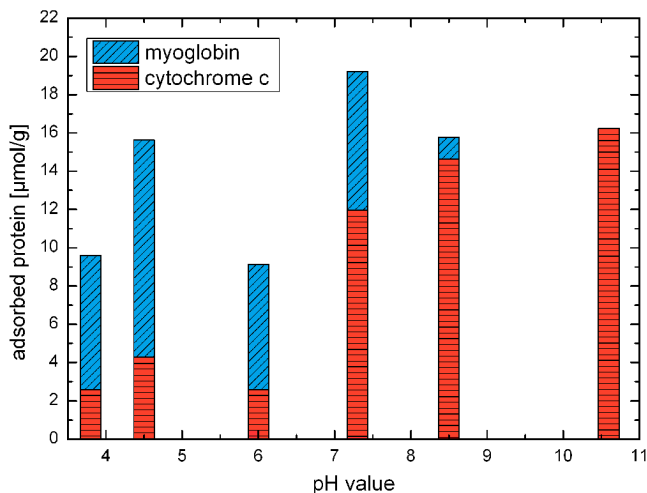


Figure 5: Proteins adsorbed to SBA-15 from a binary mixture of myoglobin and cytochrome *c* .

a binary mixture of cytochrome *c* and lysozyme. The overall height of the bar denotes the total amount of protein bound to the SBA-15 sample, while the differently dashed segments represent the shares that can be attributed to the different proteins involved. In this graph, the horizontally dashed segments represent the bound cytochrome *c*. The checkered bar represents adsorbed lysozyme. Both proteins attribute to roughly one half of the total pore loading at pH 10.6, while cytochrome *c* adsorption is slightly prevalent at lower pH values. The buffer with pH 3.8 marks an exception, where lysozyme amounts for most of the pore filling. Both proteins adsorb in mutual presence for all pH values and we do not observe any effective fractionation of the binary mixture. This is hardly surprising since both molecules are of similar size and isoelectric points.

We observe a different behavior for a mixture containing cytochrome *c* and myoglobin. As shown in Figure 5, there is a prevalence of myoglobin binding for pH 3.8, 4.5 and 6.0: The strong positive charge of the cytochrome *c* leads to high protein-protein repulsion. The adsorption of cytochrome *c* is therefore less favorable than the adsorption of myoglobin, which is much closer to its pI. This trend is reversed above the myoglobin's isoelectric point where the overall charge of the protein becomes negative i.e. , for all buffers with a pH of 7.3 and higher. The overall charge now leads to electrostatic repulsion between the silica

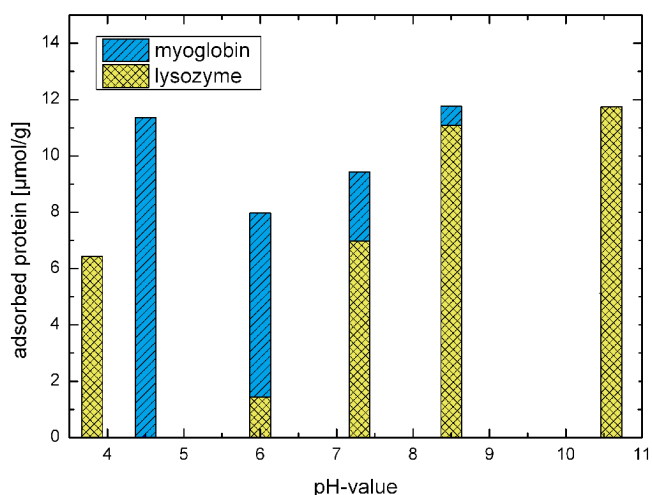


Figure 6: Proteins adsorbed to SBA-15 from a binary mixture of myoglobin and lysozyme.

and the myoglobin and consequently cytochrome *c* adsorption is favoured. Interestingly, myoglobin can still adsorb at high pH values from single protein solutions, as shown in Figure 3, but gets completely displaced at pH 10.6 when competing with cytochrome *c* . A closer look at the data reveals that not only is there no myoglobin bound to the silica particles, the observed pore loading corresponds to the entire amount of cytochrome *c* present in the initial solution, rendering the supernate devoid of this protein. This is possible because of the large specific surface and thus sorption capability of the mesoporous medium employed.

This becomes even more pronounced when comparing myoglobin with lysozyme. The data for their competitive adsorption are shown in Figure 6. We find exclusive binding of lysozyme at pH 10.6 with more than 85% of the entire lysozyme immobilised in the silica pores and exclusive and complete binding of myoglobin at pH 4.5. The buffers at intermediate pH values show a smooth transition between these extremes. Surprisingly, we find a complete inversion of this behavior at pH 3.8. About 45% of the lysozyme adsorbs to the SBA-15 while myoglobin is again completely displaced.

This is somewhat puzzling: The electroneutrality of the silica at these chemical conditions⁷³ readily explains a smaller affinity of the myoglobin to the surface. This should, however, also

apply for lysozyme whose strong positive charge should cause a considerable repulsion between the molecules and thus inhibit any considerable adsorption. It seems plausible to assume that local changes of the pH near the silica surface⁷⁹ might alter the local environment inside the pores in a way that the proteins are no longer stable, resulting in unpredictable changes of the adsorption behavior. Yet, a sound interpretation of this behavior is clearly beyond the scope of these experiments and complementary measurements in this pH-range are necessary in order to explore in detail the repeatability of this peculiar behavior.

Conclusions

We studied the competitive adsorption of lysozyme, myoglobin and cytochrome *c* to the mesoporous silica SBA-15 for a range of different pH values. Protein adsorption appears to be favoured in the vicinity of the protein's respective isoelectric point. Myoglobin and lysozyme, which differ strongly in their isoelectric points, can be effectively separated from a binary mixture if the buffer pH favours the adsorption of only one of the components. The type which shows the favoured binding to the silica can replace the one with the lower binding affinity, even though the latter would adsorb quite well from a single component mixture devoid of the strongly binding protein. This separation was not observed for cytochrome *c* and lysozyme, which are very similar in their pIs.

The observation that the bulk solution can be completely devoid of the pore-preferred protein, whereas the mesoporous medium is for certain pH-values and protein mixtures exclusively filled with the preferred species highlights that the large adsorption capabilities along with the pH-dependent adsorption selectivity might allow for the design of customized devices for protein separation in binary mixtures using the nowadays readily available bulk mesoporous media. Note, however, that the sizeable dissolution rate of mesoporous silica in the alkaline regime discussed above may be a high technological hurdle. Possibly, it can be surpassed by surface-grafting and thus by a stabilization of the silica walls against alkaline dissolution.

Albeit this will clearly necessitate additional studies on competitive adsorption and on SBA-15 stability in aqueous solutions.

While the importance of the electrostatic interaction for protein adsorption is widely known and generally accepted¹⁰, this study is to the best of our knowledge the first one to demonstrate exclusive adsorption from a binary mixture rather than adsorption of a mixed layer. We anticipate that this high adsorption selectivity of the mesoporous medium in comparison to planar surfaces is also related to the tubular, confined sorption geometry. It makes it difficult for the adsorbing proteins to avoid interacting with each other, whereas in a more conventional planar geometry, they might be able to still adsorb at nearby sites as they are not so intimately contained and forced to interact.

Therefore, we hope that our experimental findings will stimulate model calculations and computer simulation studies of protein adsorption in tubular geometries, similarly as this has been done recently for polyelectrolyte adsorption in charged cylindrical pores¹⁶ or for planar surfaces, that is in semi-infinite confined geometry.^{3,14,81}

In future experimental studies, it would be interesting to examine the pore size-dependence of pH-dependent competitive protein adsorption as well as the influence of distinct pore-size hierarchies as they are available nowadays for porous silica.⁸² Similarly as observed for adsorption⁸³ and transport^{84,85} of simple fluids, for molecular self-diffusion^{86–88} and for wetting of binary fluids⁸⁹, one can expect a strong influence of the characteristic confinement size on competitive adsorption processes of charged macromolecular systems.¹⁶ Another interesting experimental parameter to modify is the surface chemistry, either by changing the porous host material or by pore wall grafting. In particular, the study of mesoporous carbon materials^{90,91} with positively or negatively charged surface groups as well as the exploration of mesoporous alumina^{92,93} could be very interesting, because of the higher pH-stability of these materials in comparison to their silica counterparts.

Acknowledgments

We acknowledge stimulating and helpful discussions with Stefan Bommer, Tihamer Geyer, Volkhard Helms, Martin Jung, and Richard Zimmermann (Saarland University). This work has been supported by the German Research Foundation (DFG) within the graduate school 1276, 'Structure formation and transport in complex systems' (Saarbrücken) and through the collaborative research initiative SFB 986 'Tailor-Made Multi-Scale Materials Systems M3' (Hamburg) within the research area B.

References

- (1) Netz, R. R.; Joanny, J. F. Adsorption of Semiflexible Polyelectrolytes on Charged Planar Surfaces: Charge Compensation, Charge Reversal, and Multilayer Formation. *Macromolecules* **1999**, *32*, 9013–9025.
- (2) Adiga, S. P.; Jin, C.; Curtiss, L. A.; Monteiro-Riviere, N. A.; Narayan, R. J. Nanoporous Membranes for Medical and Biological Applications. *Wiley Interdiscip. Rev. Nanomed. Nanobiotechnol.* **2009**, *1*, 568–581.
- (3) Schmitt, Y.; Haehl, H.; Gilow, C.; Mantz, H.; Jacobs, K.; Leidinger, O.; Bellion, M.; Santen, L. Structural Evolution of Protein-Biofilms: Simulations and Experiments. *Biomicrofluidics* **2010**, *4*, 032201.
- (4) Felsovalyi, F.; Mangiagalli, P.; Bureau, C.; Kumar, S. K.; Banta, S. Reversibility of the Adsorption of Lysozyme on Silica. *Langmuir* **2011**, *27*, 11873–11882.
- (5) Lazzara, T. D.; Lau, K. H. A.; Abou-Kandil, A. I.; Caminade, A. M.; Majoral, J. P.; Knoll, W. Polyelectrolyte Layer-by-Layer Deposition in Cylindrical Nanopores. *ACS Nano* **2010**, *4*, 3909–3920.
- (6) Bhattacharyya, M. S.; Hiwale, P.; Piras, M.; Medda, L.; Steri, D.; Piludu, M.; Salis, A.; Monduzzi, M. Lysozyme Adsorption and Release from Ordered Mesoporous Materials. *J. Phys. Chem. C* **2010**, *114*, 19928–19934.
- (7) McLoughlin, S. Y.; Kastantin, M.; Schwartz, D. K.; Kaar, J. L. Single-Molecule Resolution of Protein Structure and Interfacial Dynamics on Biomaterial Surfaces. *Proc. Natl. Acad. Sci. U. S. A.* **2013**, *110*, 19396–19401.
- (8) Steri, D.; Monduzzi, M.; Salis, A. Ionic Strength Affects Lysozyme Adsorption and Release from SBA-15 Mesoporous Silica. *Microporous Mesoporous Mater.* **2013**, *170*, 164–172.
- (9) Meder, F.; Kaur, S.; Treccani, L.; Rezwan, K. Controlling Mixed-Protein Adsorption Layers on Colloidal Alumina Particles by Tailoring Carboxyl and Hydroxyl Surface Group Densities. *Langmuir* **2013**, *29*, 12502–12510.
- (10) Zhou, Z.; Hartmann, M. Progress in Enzyme Immobilization in Ordered Mesoporous Materials and Related applications. *Chem. Soc. Rev.* **2013**, *42*, 3894–3912.
- (11) Winkler, R. G.; Cherstvy, A. G. Strong and Weak Polyelectrolyte Adsorption onto Oppositely Charged Curved Surfaces. Polyelectrolyte Complexes In the Dispersed and Solid State I: Principles and Theory. *Adv. Polym. Sci.* **2014**, *255*, 1–56.
- (12) Kiesel, I.; Paulus, M.; Nase, J.; Tiemeyer, S.; Sternemann, C.; Ruester, K.; Wirkert, F. J.; Mende, K.; Buening, T.; Tolan, M. Temperature-Driven Adsorption and Desorption of Proteins at Solid-Liquid Interfaces. *Langmuir* **2014**, *30*, 2077–2083.
- (13) Retamal, M. J.; Cisternas, M. A.; Gutierrez-Maldonado, S. E.; Perez-Acle, T.; Seifert, B.; Busch, M.; Huber, P.; Volkmann, U. G. Towards Bio-silicon Interfaces: Formation of an Ultra-Thin Self-Hydrated Artificial Membrane Composed of Dipalmitoylphosphatidylcholine (DPPC) and Chitosan Deposited in High Vacuum from the Gas-Phase. *J. Chem. Phys.* **2014**, *141*, 104201–104201.
- (14) Hildebrand, N.; Koppen, S.; Derr, L.; Li, K. B.; Koleini, M.; Rezwan, K.; Ciac-

- chi, L. C. Adsorption Orientation and Binding Motifs of Lysozyme and Chymotrypsin on Amorphous Silica. *J. Phys. Chem. C* **2015**, *119*, 7295–7307.
- (15) Huber, P. Soft Matter in Hard Confinement: Phase Transition Thermodynamics, Structure, Texture, Diffusion and Flow in Nanoporous Media. *J. Phys. : Cond. Matt.* **2015**, *27*, 103102.
- (16) de Carvalho, S. J.; Metzler, R.; Cherstvy, A. G. Inverted Critical Adsorption of Polyelectrolytes in Confinement. *Soft Matter* **2015**, *11*, 4430–4443.
- (17) Meissner, J.; Prause, A.; Di Tommaso, C.; Bharti, B.; Findenegg, G. H. Protein Immobilization in Surface-Functionalized SBA-15: Predicting the Uptake Capacity from the Pore Structure. *J. Phys. Chem. C* **2015**, *119*, 2438–2446.
- (18) Zimmermann, R.; Eyrich, S.; Ahmad, M.; Helms, V. Protein Translocation across the ER Membrane. *BBA-Biomembranes* **2011**, *1808*, 912–924.
- (19) Mahendran, K. R.; Lamichhane, U.; Romero-Ruiz, M.; Nussberger, S.; Winterhalter, M. Polypeptide Translocation Through the Mitochondrial TOM Channel: Temperature-Dependent Rates at the Single-Molecule Level. *J. Phys. Chem. Lett.* **2013**, *4*, 78–82.
- (20) Fratzl, P.; Weinkamer, R. Nature's Hierarchical Materials. *Prog. Mater. Sci.* **2007**, *52*, 1263–1334.
- (21) Zlotnikov, I.; Werner, P.; Blumtritt, H.; Graff, A.; Dauphin, Y.; Zolotoyabko, E.; Fratzl, P. A Perfectly Periodic Three-Dimensional Protein/Silica Mesoporous Structure Produced by an Organism. *Adv. Mater.* **2014**, *26*, 1682–1687.
- (22) Javidpour, L.; Tabar, M. R. R.; Sahimi, M. Molecular Simulation of Protein Dynamics in Nanopores. I. Stability and Folding. *J. Chem. Phys.* **2008**, *128*, 115105.
- (23) Javidpour, L.; Tabar, M. R. R.; Sahimi, M. Molecular Simulation of Protein Dynamics in Nanopores. II. Diffusion. *J. Chem. Phys.* **2009**, *130*, 085105.
- (24) Firnkes, M.; Pedone, D.; Knezevic, J.; Doeblinger, M.; Rant, U. Electrically Facilitated Translocations of Proteins through Silicon Nitride Nanopores: Conjoint and Competitive Action of Diffusion, Electrophoresis, and Electroosmosis. *Nano Lett.* **2010**, *10*, 2162–2167.
- (25) Lee, P.-H.; Helms, V.; Geyer, T. Coarse-Grained Brownian Dynamics Simulations of Protein Translocation through Nanopores. *J. Chem. Phys.* **2012**, *137*, 145105.
- (26) Plesa, C.; Kowalczyk, S. W.; Zinsmeister, R.; Grosberg, A. Y.; Rabin, Y.; Dekker, C. Fast Translocation of Proteins through Solid State Nanopores. *Nano Lett.* **2013**, *13*, 658–663.
- (27) Mihovilovic, M.; Hagerty, N.; Stein, D. Statistics of DNA Capture by a Solid-State Nanopore. *Phys. Rev. Lett.* **2013**, *110*, 028102.
- (28) Hartmann, M. Ordered Mesoporous Materials for Bioadsorption and Biocatalysis. *Chem. Mater.* **2005**, *17*, 4577–4593.
- (29) Fried, D. I.; Brieler, F. J.; Froeba, M. Designing Inorganic Porous Materials for Enzyme Adsorption and Applications in Biocatalysis. *ChemCatChem* **2013**, *5*, 862–884.
- (30) Chayen, N. E.; Saridakis, E.; Sear, R. P. Experiment and Theory for Heterogeneous Nucleation of Protein Crystals in a Porous Medium. *Proc. Natl. Acad. Sci. U. S. A.* **2006**, *103*, 597–601.
- (31) van Meel, J. A.; Sear, R. P.; Frenkel, D. Design Principles for Broad-Spectrum Protein-Crystal Nucleants with Nanoscale Pits. *Phys. Rev. Lett.* **2010**, *105*, 205501.
- (32) Yang, S. Y.; Ryu, I.; Kim, H. Y.; Kim, J. K.; Jang, S. K.; Russell, T. P. Nanoporous Membranes with Ultrahigh Selectivity and Flux

- for the Filtration of Viruses. *Adv. Mater.* **2006**, *18*, 709–712.
- (33) Slowing, I.; Trewyn, B.; Lin, V. Mesoporous Silica Nanoparticles for Intracellular Delivery of Membrane-Impermeable Proteins. *J. Am. Chem. Soc.* **2007**, *129*, 8845–8849.
- (34) Seker, E.; Berdichevsky, Y.; Staley, K. J.; Yarmush, M. L. Microfabrication-Compatible Nanoporous Gold Foams as Biomaterials for Drug Delivery. *Adv. Healthcare Mater.* **2012**, *1*, 172–176.
- (35) Xue, M.; Findenegg, G. H. Lysozyme as a pH-Responsive Valve for the Controlled Release of Guest Molecules from Mesoporous Silica. *Langmuir* **2012**, *28*, 17578–17584.
- (36) Kurtulus, O.; Daggumati, P.; Seker, E. Molecular Release from Patterned Nanoporous Gold Thin Films. *Nanoscale* **2014**, *6*, 7062–7071.
- (37) Argyo, C.; Weiss, V.; Braeuchle, C.; Bein, T. Multifunctional Mesoporous Silica Nanoparticles as a Universal Platform for Drug Delivery. *Chem. Mater.* **2014**, *26*, 435–451.
- (38) Niedermayer, S.; Weiss, V.; Herrmann, A.; Schmidt, A.; Datz, S.; Mueller, K.; Wagner, E.; Bein, T.; Braeuchle, C. Multifunctional Polymer-Capped Mesoporous Silica Nanoparticles for pH-Responsive Targeted Drug Delivery. *Nanoscale* **2015**, *7*, 7953–7964.
- (39) Graubner, G.; Rengarajan, G. T.; Anders, N.; Sonnenberger, N.; Enke, D.; Beiner, M.; Steinhart, M. Morphology of Porous Hosts Directs Preferred Polymorph Formation and Influences Kinetics of Solid/Solid Transitions of Confined Pharmaceuticals. *Cryst. Growth & Design* **2014**, *14*, 78–86.
- (40) Janshoff, A.; Dancil, K. P. S.; Steinem, C.; Greiner, D. P.; Lin, V. S. Y.; Gurtner, C.; Motesharei, K.; Sailor, M. J.; Ghadiri, M. R. Macroporous p-Type Silicon Fabry-Perot Layers. Fabrication, Characterization, and Applications in Biosensing. *J. Am. Chem. Soc.* **1998**, *120*, 12108–12116.
- (41) Kilian, K. A.; Boecking, T.; Gooding, J. J. The Importance of Surface Chemistry in Mesoporous Materials: Lessons from Porous Silicon Biosensors. *Chem. Commun.* **2009**, 630–640.
- (42) Guan, B.; Magenau, A.; Kilian, K. A.; Ciampi, S.; Gaus, K.; Reece, P. J.; Gooding, J. J. Mesoporous Silicon Photonic Crystal Microparticles: Towards Single-Cell Optical Biosensors. *Faraday Discuss.* **2011**, *149*, 301–317.
- (43) Chen, M. Y.; Klunk, M. D.; Diep, V. M.; Sailor, M. J. Electric-Field-Assisted Protein Transport, Capture, and Interferometric Sensing in Carbonized Porous Silicon Films. *Adv. Mater.* **2011**, *23*, 4537–4542.
- (44) Fan, J.; Deng, X.; Gallagher, J. W.; Huang, H.; Huang, Y.; Wen, J.; Ferrari, M.; Shen, H.; Hu, Y. Monitoring the Progression of Metastatic Breast Cancer on Nanoporous Silica Chips. *Philos. Trans. Roy. Soc. A* **2012**, *370*, 2433–2447.
- (45) Boecking, T.; Kilian, K. A.; Reece, P. J.; Gaus, K.; Gal, M.; Gooding, J. J. Biofunctionalization of Free-Standing Porous Silicon Films for Self-Assembly of Photonic devices. *Soft Matter* **2012**, *8*, 360–366.
- (46) Eijkel, J. C. T.; van den Berg, A. Nanofluidics: What Is It and What Can We Expect from It? *Microfluid. Nanofluid.* **2005**, *1*, 249.
- (47) Gruener, S.; Huber, P. Spontaneous Imbibition Dynamics of an n-Alkane in Nanopores: Evidence of Meniscus Freezing and Monolayer Sticking. *Phys. Rev. Lett.* **2009**, *103*, 174501.
- (48) Gruener, S.; Sadjadi, Z.; Hermes, H. E.; Kityk, A. V.; Knorr, K.; Egelhaaf, S. U.; Rieger, H.; Huber, P. Capillary Rise Dynamics of Liquid Hydrocarbons in Mesoporous Silica as Explored by Gravimetry, Optical and Neutron Imaging: Nano-Rheology and Determination of Pore-Size Distributions from the Shape

- of Imbibition Fronts. *Coll. Surf. A* **2015**, 10.1016/j.colsurfa.2015.09.055.
- (49) Dittrich, P. S.; Manz, A. Lab-on-a-Chip: Microfluidics in Drug Discovery. *Nat. Rev. Drug Discov.* **2006**, 5, 210–218.
- (50) Stone, H. A.; Stroock, A. D.; Ajdari, A. Engineering Flows in Small Devices: Microfluidics toward a Lab-on-a-Chip. *Ann. Rev. Fluid Mech.* **2004**, 36, 381.
- (51) Hu, Y.; Gopal, A.; Lin, K.; Peng, Y.; Tasciotti, E.; Zhang, X. J.; Ferrari, M. Microfluidic Enrichment of Small Proteins from Complex Biological Mixture on Nanoporous Silica Chip. *Biomicrofluidics* **2011**, 5, 013410–013410.
- (52) Yazdi, S. H.; White, I. M. A Nanoporous Optofluidic Microsystem for Highly Sensitive and Repeatable Surface Enhanced Raman Spectroscopy Detection. *Biomicrofluidics* **2012**, 6, 014105.
- (53) Bocquet, L.; Tabeling, P. Physics and Technological Aspects of Nanofluidics. *Lab on a chip* **2014**, 14, 3143–58.
- (54) Xue, Y.; Markmann, J.; Duan, H.; Weissmueller, J.; Huber, P. Switchable Imbibition in Nanoporous Gold. *Nat. Commun.* **2014**, 5, 4237.
- (55) Causserand, C.; Kara, Y.; Aimar, P. Protein Fractionation Using Selective Adsorption on Clay Surface before Filtration. *J. Membr. Sci.* **2001**, 186, 165–181.
- (56) Sun, Z.; Deng, Y.; Wei, J.; Gu, D.; Tu, B.; Zhao, D. Hierarchically Ordered Macro-/Mesoporous Silica Monolith: Tuning Macropore Entrance Size for Size-Selective Adsorption of Proteins. *Chem. Mater.* **2011**, 23, 2176–2184.
- (57) Qian, K.; Zhou, L.; Zhang, J.; Lei, C.; Yu, C. A Combo-Pore Approach for the Programmable Extraction of Peptides/Proteins. *Nanoscale* **2014**, 6, 5121–5125.
- (58) Yue, Q.; Li, J.; Luo, W.; Zhang, Y.; Elzatahry, A. A.; Wang, X.; Wang, C.; Li, W.; Cheng, X.; Alghamdi, A. et al. An Interface Coassembly in Biliquid Phase: Toward Core-Shell Magnetic Mesoporous Silica Microspheres with Tunable Pore Size. *J. Am. Chem. Soc.* **2015**, 137, 13282–9.
- (59) Striemer, C. C.; Gaborski, T. R.; McGrath, J. L.; Fauchet, P. M. Charge- and Size-based Separation of Macromolecules using Ultrathin Silicon Membranes. *Nature* **2007**, 445, 749–753.
- (60) Uehara, H.; Kakiage, M.; Sekiya, M.; Sakuma, D.; Yamonobe, T.; Takano, N.; Barraud, A.; Meurville, E.; Ryser, P. Size-Selective Diffusion in Nanoporous but Flexible Membranes for Glucose Sensors. *ACS Nano* **2009**, 3, 924–932.
- (61) Katiyar, A.; Pinto, N. G. Visualization of Size-Selective Protein Separations on Spherical Mesoporous Silicates. *Small* **2006**, 2, 644–648.
- (62) Fujii, E.; Ohkubo, M.; Tsuru, K.; Hayakawa, S.; Osaka, A.; Kawabata, K.; Bonhomme, C.; Babonneau, F. Selective Protein Adsorption Property and Structure of Nano-crystalline Hydroxy-Carbonate Apatite. *Acta Biomater.* **2006**, 2, 69–74.
- (63) Segel, D. J.; Fink, A. L.; Hodgson, K. O.; Doniach, S. Protein Denaturation: A Small-angle X-ray Scattering Study of the Ensemble of Unfolded States of Cytochrome c. *Biochem.* **1998**, 37, 12443–12451.
- (64) Sang, L.-C.; Vinu, A.; Coppens, M.-O. General Description of the Adsorption of Proteins at Their Iso-electric Point in Nanoporous Materials. *Langmuir* **2011**, 27, 13828–13837.
- (65) Zhao, D. Y.; Feng, J. L.; Huo, Q. S.; Melosh, N.; Fredrickson, G. H.; Chmelka, B. F.; Stucky, G. D. Triblock Copolymer Syntheses of Mesoporous Silica with Periodic 50 to 300 Angstrom Pores. *Science* **1998**, 279, 548–552.

- (66) Cole, M. W.; Saam, W. F. Excitation Spectrum and Thermodynamic Properties of Liquid-Film in Cylindrical Pores. *Phys. Rev. Lett.* **1974**, *32*, 985–988.
- (67) Saam, W. F.; Cole, M. W. Excitations and Thermodynamics for Liquid-Helium Films. *Phys. Rev. B* **1975**, *11*, 1086–1105.
- (68) Imperor-Clerc, M.; Davidson, P.; Davidson, A. Existence of a Microporous Corona around the Mesopores of Silica-Based SBA-15 Materials Templated by Triblock Copolymers. *J. Am. Chem. Soc.* **2000**, *122*, 11925–11933.
- (69) Hofmann, T.; Wallacher, D.; Huber, P.; Birringer, R.; Knorr, K.; Schreiber, A.; Findenegg, G. H. Small-Angle X-Ray Diffraction of Kr in Mesoporous Silica: Effects of Microporosity and Surface Roughness. *Phys. Rev. B* **2005**, *72*, 064122.
- (70) Zickler, G. A.; Jaehnert, S.; Wagermaier, W.; Funari, S. S.; Findenegg, G. H.; Paris, O. Physisorbed Films in Periodic Mesoporous Silica Studied by In-Situ Synchrotron Small-Angle Diffraction. *Phys. Rev. B* **2006**, *73*, 184109.
- (71) Rosenholm, J. M.; Linden, M. Zeta Potential of Microfluidic Substrates: 1. Theory, Experimental Techniques, and Effects on Separations *Journal of Controlled Release* **2008**, *128*, 157–164.
- (72) Kirby, B. J.; Hasselbrink, E. F. Towards Establishing Structure-Activity Relationships for Mesoporous Silica in Drug Delivery Applications *Electrophoresis* **2004**, *25*, 187–202.
- (73) Essa, H.; Magner, E.; Cooney, J.; Hodnett, B. K. Influence of pH and Ionic Strength on the Adsorption, Leaching and Activity of Myoglobin Immobilized onto Ordered Mesoporous Silicates. *J. Mol. Catal. B: Enzym.* **2007**, *49*, 61–68.
- (74) Moerz, S. T.; Huber, P. Protein Adsorption into Mesopores: A Combination of Electrostatic Interaction, Counterion release and Van-der-Waals forces. *Langmuir* **2013**, *30*, 2729–2737.
- (75) Zhang, X.; Wang, J.; Wu, W.; Qian, S.; Man, Y. Immobilization and Electrochemistry of Cytochrome *c* on Amino-Functionalized Mesoporous Silica Thin Films. *Electrochem. Commun.* **2007**, *9*, 2098–2104.
- (76) Vinu, A.; Murugesan, V.; Tangermann, O.; Hartmann, M. Adsorption of Cytochrome *c* on Mesoporous Molecular Sieves: Influence of pH, Pore Diameter, and Aluminum incorporation. *Chem. Mater.* **2004**, *16*, 3056–3065.
- (77) Oellerich, S.; Wackerbarth, H.; Hildebrandt, P. Spectroscopic Characterization of Nonnative Conformational States of Cytochrome *c*. *J. Phys. Chem. B* **2002**, *106*, 6566–6580.
- (78) Kraning, C. M.; Benz, T. L.; Bloome, K. S.; Campanello, G. C.; Fahrenbach, V. S.; Mistry, S. A.; Hedge, C. A.; Clevenger, K. D.; Gligorich, K. M.; Hopkins, T. A. et al. Determination of Surface Coverage and Orientation of Reduced Cytochrome *c* on a Silica Surface with Polarized ATR Spectroscopy. *J. Phys. Chem. C* **2007**, *111*, 13062–13067.
- (79) Hartvig, R. A.; van de Weert, M.; Ostergaard, J.; Jorgensen, L.; Jensen, H. Protein Adsorption at Charged Surfaces: The Role of Electrostatic Interactions and Interfacial Charge Regulation. *Langmuir* **2011**, *27*, 2634–2643.
- (80) Pham, A. L.-T.; Sedlak, D. L.; Doyle, F. M. Dissolution of Mesoporous Silica Supports in Aqueous Solutions: Implications for Mesoporous Silica-Based Water Treatment Processes. *Appl. Catal. B* **2012**, *126*, 258–264.
- (81) Szott, L. M.; Horbett, T. A. Protein Interactions with Surfaces: Computational Ap-

- proaches and Repellency. *Curr. Opin. Chem. Biol.* **2011**, *15*, 683–689.
- (82) Inayat, A.; Reinhardt, B.; Uhlig, H.; Einicke, W. D.; Enke, D. Silica Monoliths with Hierarchical Porosity Obtained From Porous Glasses. *Chem. Soc. Rev.* **2013**, *42*, 3753–3764.
- (83) Huber, P.; Knorr, K. Adsorption-Desorption Isotherms and X-Ray Diffraction of Ar Condensed into a Porous Glass Matrix. *Phys. Rev. B* **1999**, *60*, 12657–12665.
- (84) Gruener, S.; Huber, P. Imbibition in Mesoporous Silica: Rheological Concepts and Experiments on Water and a Liquid Crystal. *J. Phys. : Cond. Matt.* **2011**, *23*, 184109.
- (85) Kriel, F. H.; Sedev, R.; Priest, C. Capillary Filling of Nanoscale Channels and Surface Structure. *Isr. J. Chem.* **2014**, *54*, 1519–1532.
- (86) Kusmin, A.; Gruener, S.; Henschel, A.; Holderer, O.; Allgaier, J.; Richter, D.; Huber, P. Evidence of a Sticky Boundary Layer in Nanochannels: A Neutron Spin Echo Study of n-Hexatriacontane and Poly(ethylene oxide) Confined in Porous Silicon. *J. Phys. Chem. Lett.* **2010**, *1*, 3116–3121.
- (87) Hofmann, T.; Wallacher, D.; Mayorova, M.; Zorn, R.; Frick, B.; Huber, P. Molecular Dynamics of n-Hexane: A Quasi-Elastic Neutron Scattering Study on the Bulk and Spatially Nanochannel-Confined Liquid. *J. Chem. Phys.* **2012**, *136*, 124505.
- (88) Valiullin, R.; Kaerger, J.; Glaeser, R. Correlating Phase Behaviour and Diffusion in Mesopores: Perspectives Revealed by Pulsed Field Gradient NMR. *Phys. Chem. Chem. Phys.* **2009**, *11*, 2833–2853.
- (89) Woywod, D.; Schoen, M. Phase Behavior of Confined Symmetric Binary Mixtures. *Phys. Rev. E* **2003**, *67*, 026122.
- (90) Presser, V.; Heon, M.; Gogotsi, Y. Carbide-Derived Carbons - From Porous Networks to Nanotubes and Graphene. *Adv. Funct. Mater.* **2011**, *21*, 810–833.
- (91) Liu, R.-L.; Yin, F.-Y.; Zhang, J.-F.; Zhang, J.; Zhang, Z.-Q. Intestine-Like Micro/Mesoporous Carbon Built of Chemically Modified Banana Peel for Size-Selective Separation of Proteins. *RSC Adv.* **2014**, *4*, 21465–21470.
- (92) Lu, S.; An, Z.; He, J.; Li, B. Hierarchically-Structured Immobilized Enzyme Displaying the Multi-Functions of Bio-Membranes. *J. Mater. Chem.* **2012**, *22*, 3882–3888.
- (93) El-Safty, S. A.; Shenashen, M. A.; Khairy, M. Bioadsorption of Proteins on Large Mesocage-Shaped Mesoporous Alumina Monoliths. *Coll. Surf. B* **2013**, *103*, 288–297.

Graphical TOC Entry

